

Oscillations of the Orbital Magnetic Moment due to *d*-Band Quantum Well States

M. Dąbrowski,^{1,*} T. R. F. Peixoto,¹ M. Pazgan,¹ A. Winkelmann,¹ M. Cinal,² T. Nakagawa,³ Y. Takagi,³ T. Yokoyama,³ F. Bisio,⁴ U. Bauer,¹ F. Yildiz,¹ M. Przybylski,^{1,5} and J. Kirschner^{1,6}

¹Max-Planck-Institut für Mikrostrukturphysik, 06120 Halle, Germany

²Institute of Physical Chemistry, Polish Academy of Sciences, 01-224 Warsaw, Poland

³Institute for Molecular Science, Myodaiji-cho, Okazaki, Aichi 444-8585, Japan

⁴CNR-SPIN Corso Perrone 24, I-16152 Genova, Italy

⁵Faculty of Physics and Applied Computer Science, and Academic Centre for Materials and Nanotechnology, AGH University of Science and Technology, 30-059 Kraków, Poland

⁶Naturwissenschaftliche Fakultät II, Martin-Luther-Universität Halle-Wittenberg, 06120 Halle, Germany

(Received 7 February 2014; revised manuscript received 1 July 2014; published 6 August 2014)

The effect of electron confinement on the magnetocrystalline anisotropy of ultrathin bcc Fe films is explored by combining photoemission spectroscopy, x-ray magnetic circular dichroism, and magneto-optical Kerr effect measurements. Pronounced thickness-dependent variations in the magnetocrystalline anisotropy are ascribed to periodic changes in the density of states at the Fermi level, induced by quantization of d_{xz} , d_{yz} out-of-plane orbitals. Our results reveal a direct correlation between quantum well states, the orbital magnetic moment, and the magnetocrystalline anisotropy.

DOI: 10.1103/PhysRevLett.113.067203

PACS numbers: 75.30.Gw, 73.21.Fg, 75.70.Tj, 79.60.-i

In thin films, electron motion can be confined by the potential barriers at the interfaces, leading to the formation of quantum well states (QWS). Recently, increasing attention has been paid to the quantum confinement of spin-polarized electrons, motivated by both fundamental questions and applications in spintronics. While numerous studies report the spin-dependent confinement of nearly free *sp* electrons [1–3], QWS from *d* electrons are still poorly explored. The short lifetime and mean-free path of *d* states make them, in fact, elusive to experimental detection [4]. The confinement of *d* electrons is particularly interesting in ferromagnetic transition-metal films where the *d* electrons themselves largely govern the magnetic properties. Correspondingly, QWS in the vicinity of the Fermi level E_F are expected to modulate the magnetocrystalline anisotropy energy (MAE) [5]. Indeed, an oscillatory magnetocrystalline anisotropy as a function of the overlayer thickness has been observed experimentally for bcc Fe and fcc Co films [6–8] and ascribed to the quantization of *d* states. Because of its potential to simultaneously control the magnetization direction [8] and the tunneling magnetoresistance ratio [9], spin-polarized confinement in ferromagnetic films is of great technological interest.

In this Letter, we experimentally demonstrate the direct correlation between oscillations of the in-plane MAE and the density of states at the Fermi level due to majority QWS of Δ_5 character in ultrathin bcc Fe films. We further show that the key factor that governs the oscillations of the MAE is a change of the *in-plane* component of the orbital magnetic moment. Our results yield the intuitive picture that the quantization of the wave vector perpendicular to the film surface arises due to the confinement of the electron

motion in out-of-plane orbitals, which in turn, results in changes of the in-plane orbital magnetic moment.

All the experiments were performed in ultrahigh vacuum systems, with base pressure below 1×10^{-10} mbar. Two types of crystals, flat Ag(001) and vicinal Ag(116), were employed. The substrates were cleaned by cycles of ion bombardment (Ar^+ , 1 keV) and subsequent annealing at 775 K. The chemical cleanness and surface roughness of the substrates were verified by Auger electron spectroscopy and low-energy electron diffraction. The bcc Fe films were grown at room temperature by molecular beam epitaxy as either wedge-shaped or constant-thickness samples, depending on the demands of particular experiments. After the growth process, the Fe films were annealed at 500 K in order to improve the surface morphology [10,11]. We limit our discussion to effects caused solely by QWS so that we focus here on Fe thicknesses above the spin reorientation transition (SRT), i.e., above 6 ML of Fe [12] (see the Supplemental Material [13]).

The symmetry character and spin polarization of the QWS were determined by polarization-dependent and spin-resolved photoemission spectroscopy (PES). The magnetic anisotropy was determined via magneto-optical Kerr effect (MOKE) measurements, while the orbital magnetic moment was deduced by means of x-ray magnetic circular dichroism (XMCD). The photoemission spectra were recorded at 150 and 300 K, in normal emission, with the incident light polarization either perpendicular (*s* polarization) or parallel (*p* polarization) to the optical plane [Fig. 1(a)]. The photoelectron spin was measured by an electron spin analyzer based on exchange scattering at Fe/W(001) [14] [Fig. 1(a)].

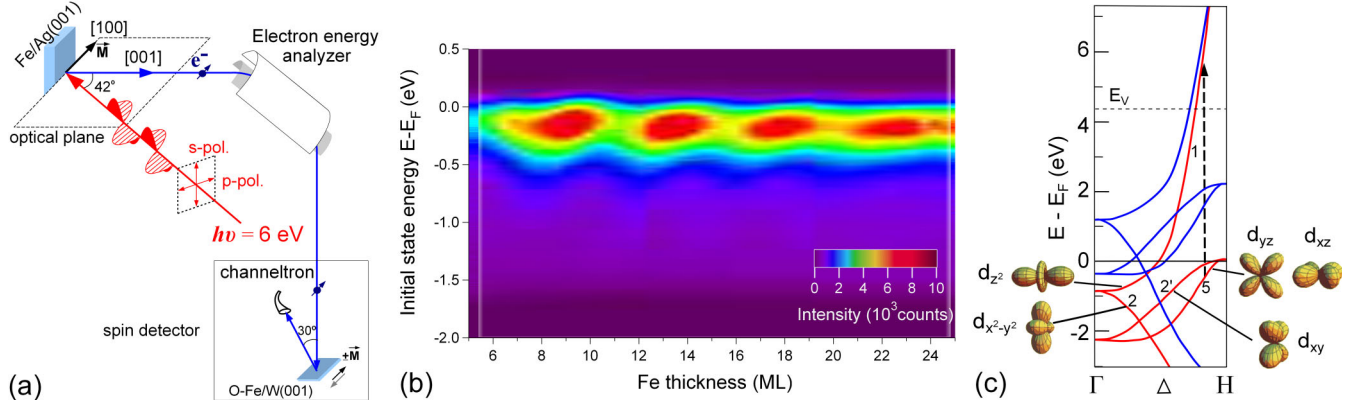


FIG. 1 (color online). (a) Schematics of the spin-polarized PES experiment. (b) Thickness- and energy-dependent photoemission intensity distribution of Fe/Ag(001) at 300 K, for s -polarized incident light, with energy $h\nu = 6$ eV. The intensity peaks below E_F correspond to the resonant transition depicted by a vertical arrow in the (c) spin-resolved bulk Fe(001) band structure [15,16]. The curves in red (blue) are the majority (minority) spin-split bands. The initial states are QWS of the majority-spin Δ_5 band near the H point, which mainly consists of the doubly degenerated d_{xz} , d_{yz} orbitals.

The thickness-dependent photoemission spectra obtained with s -polarized incident light are shown in Fig. 1(b). The oscillations of the PES intensity with increasing Fe thickness indicate the formation of QWS in the vicinity of the Fermi level E_F . In normal emission [Fig. 1(a)], the dipole selection rules allow transitions from Δ_1 (of sp , d_{z^2} orbital character) and Δ_5 (of d_{xz} , d_{yz} orbital character) initial states with incident p -polarized light, whereas only from Δ_5 states for s -polarized light [17,18]. Since the QWS can be observed for both polarizations, they originate from the Δ_5 band, consisting of the doubly degenerated d_{xz} and d_{yz} out-of-plane orbitals [19]. Additional information about the electronic band forming QWS can be deduced from the period L of the photoemission intensity oscillations [20]. The period L (in ML) is directly related to the wave vector of the confined electronic state as $L = (2\pi/a)(k_{\text{env}})^{-1}$, where a is the lattice constant and k_{env} is defined as the wave vector spanning the crossing point of the electronic band at a given energy and the nearest high-symmetry point of the Brillouin zone (BZ) [21]. The period of the photoemission intensity oscillations in our experiment $L = 4.5 \pm 0.3$ ML (at 0.2 eV below E_F) corresponds to $k_{\text{env}} = 0.22 \pm 0.01 k_{\text{BZ}}$ (where $k_{\text{BZ}} = 2\pi/a$ is the wave vector corresponding to the H point at the Brillouin zone boundary). For a photon energy of 6 eV, a corresponding nearly resonant electronic transition from d_{xz} , d_{yz} majority-spin state to d_{z^2} state is depicted by a vertical arrow in Fig. 1(c). By looking at the bulk electronic structure of bcc Fe [Fig. 1(c)], we can conclude that the observed QWS of Δ_5 symmetry are expected to be dominated by majority-spin electrons (corresponding to $k_{\text{env}} \approx 0.2 k_{\text{BZ}}$) rather than minority-spin electrons (corresponding to $k_{\text{env}} \approx 0.5 k_{\text{BZ}}$).

Since the spin polarization of the photoelectrons in our scattering geometry is mainly determined by the exchange splitting and spin-orbit coupling of initial states [22], the spin-resolved photoemission measurements allow us to

assess the magnetic properties of the confined d_{xz} , d_{yz} orbitals. Spin-resolved PES intensity profiles were measured as a function of the Fe film thickness, at fixed energy 0.2 eV below E_F (not shown here), as well as spin-resolved PES spectra at thicknesses corresponding to the maxima and minima of the PES intensity modulations. Typical spin-resolved PES spectra recorded at 300 K, for thicknesses $t_{\text{Fe}} = 9$ ML (PES intensity maximum) and $t_{\text{Fe}} = 11$ ML (PES intensity minimum), are shown respectively in Figs. 2(a) and 2(b). In these graphs, the partial intensities of majority I_{\uparrow} and minority I_{\downarrow} photoelectrons, together with the corresponding spin polarization defined as $P = (I_{\uparrow} - I_{\downarrow}) / (I_{\uparrow} + I_{\downarrow})$, are depicted as a function of initial state energy. The spectra show predominantly majority-spin character, as expected for low photon energies [23,24]. The spin polarization reaches a maximum of 0.45 at the energy of 0.2 eV below E_F , in good agreement with previous reports on the Fe(001) surface [23,25]. The slight increase of spin polarization approaching 0.2 eV below E_F confirms the majority-spin character of the probed initial states. However, there is no significant difference in the spin polarization between maxima and minima of the PES intensity. In fact, both majority (red-up triangles) and minority (blue-down triangles) partial intensities decrease to 41% of their maximum intensities, from $t_{\text{Fe}} = 9$ to 11 ML, showing that the probed initial state is a mixture of majority and minority states. A significant spin mixing in ferromagnetic films can occur in the proximity of hybridization points due to the spin-orbit interaction [26,27]. The origin of the spin mixing in the present QWS is, however, not clear, since there are no such hybridization points across the Δ_5 band in the vicinity of the H point [28].

In order to study the effect of QWS on the magnetic anisotropy, we performed MOKE measurements on Fe films grown on the Ag(116) vicinal surface. Deposition of the ferromagnetic film on the vicinal surface introduces an

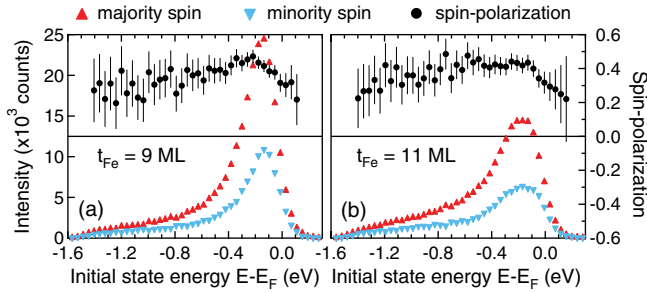


FIG. 2 (color online). Spin-resolved PES spectra for (a) $t_{\text{Fe}} = 9$ ML and (b) 11 ML, PES intensity maximum and minimum, respectively. The red-up (blue-down) triangles correspond to the majority (minority) spin partial intensity, with respect to the in-plane remanent magnetization direction, measured with s -polarized light, at 300 K. Both spin-channel intensities vary equally with thickness, leading to a monotonic behavior of the spin polarization.

additional in-plane uniaxial magnetic anisotropy and allows us to measure split hysteresis loops, characterized by a shift field H_s . The value of H_s is a measure of the in-plane uniaxial magnetic anisotropies and allows us to determine the period and amplitude of magnetic anisotropy oscillations with high accuracy [6,29]. Split hysteresis loops were recorded by *in situ* MOKE in the longitudinal configuration using a laser diode of wavelength 670 nm at fixed incidence angle $\varphi = 30^\circ$ measured with respect to the sample normal. The shift fields H_s , evaluated from split hysteresis loops measured at $T = 5$ K, are plotted in Fig. 3 as a function of Fe film thickness. Pronounced oscillations of H_s with a period of $L = 5.5 \pm 0.3$ ML are observed, in agreement with previous reports [6,7]. A larger H_s value means that more magnetic field has to be applied perpendicular to the step edges to align the magnetization with the external field and, therefore, corresponds to higher magnetic anisotropy. In Fig. 3, H_s obtained from MOKE measurements is compared with the photoemission intensity at 0.2 eV below E_F .

The comparison of MOKE and PES measurements indicates that both oscillatory phenomena are correlated. The contributions to the MAE due to quantization are expected to reach a maximum for Fe thicknesses at which the QWS cross E_F [30]. Because of the thickness dispersion of the QWS, the period of the PES intensity oscillations is energy dependent. Therefore, the Fe thicknesses at which the QWS cross E_F are different from the thicknesses at which the PES intensity peaks appear at 0.2 eV below E_F . Accordingly, there is a shift in thickness of the PES peaks with respect to the maxima of H_s (Fig. 3). It is worth noting that the dispersion of QWS is less pronounced in our experiment [Fig. 1(b)] than in the typical QWS from sp bands [20]. This confirms that the wave functions observed by us in PES are built of localized d orbitals that form narrow energy bands.

Although a mutual relation between oscillatory photoemission intensity and shift field H_s appears straightforward,

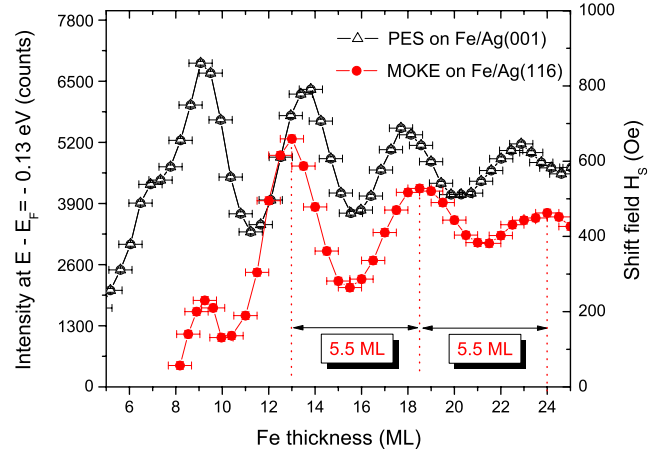


FIG. 3 (color online). Thickness dependence of the photoemission intensity at the d -QWS energy $E - E_F = -0.2$ eV at $T = 300$ K and of the shift field H_s obtained from MOKE measurements at $T = 5$ K.

we cannot completely exclude the possibility that a band with other spatial symmetry contributes to the oscillatory magnetic anisotropy [31]. It is, therefore, desirable to explore the microscopic mechanism of the magnetic anisotropy oscillations in more detail. As proposed by Bruno [32], a direct connection between orbital moment anisotropy and magnetocrystalline anisotropy can exist [33]. In this respect, the orbital moment provides a link between electronic orbitals and magnetic anisotropy. Thus, it is essential to verify how the formation of d -QWS influences the orbital magnetic moment. For this purpose, XMCD measurements were performed at the bending magnet station beam line 4B at the UVSOR-II in Institute for Molecular Science, Japan [34]. The schematic view of the XMCD experiment on Fe/Ag(116) is shown in Fig. 4(a). All the absorption spectra were taken in saturation by applying a magnetic field of ± 4 T, while leaving the photon helicity σ^- unchanged. The x-ray propagation direction and the magnetic field direction are always collinear in the present setup (see the Supplemental Material [13]). Three geometries of the applied magnetic field were used: (i) perpendicular to the macroscopic sample plane ($\theta = 0^\circ$), (ii) perpendicular to the step edges at $\theta = 55^\circ$, and (iii) parallel to the step edges at $\theta = 55^\circ$. The XMCD data set of three independent incidence angles allows us to evaluate the orbital moment component perpendicular to the sample plane and the in-plane orbital moment components along the step edges ($m_{\text{orb}}^{\parallel}$) and perpendicular to the step edges (m_{orb}^{\perp}) [35].

Our results reveal that periodic changes of the orbital magnetic moment occur only for the in-plane components m_{orb}^{\perp} and $m_{\text{orb}}^{\parallel}$ (Supplemental Material [13]); i.e., according to the intuitive picture [36], they arise mostly from out-of-plane d_{xz} , d_{yz} orbitals [Fig. 4(a)]. In contrast, the orbital moment component perpendicular to the sample plane decreases monotonically with increasing Fe thickness

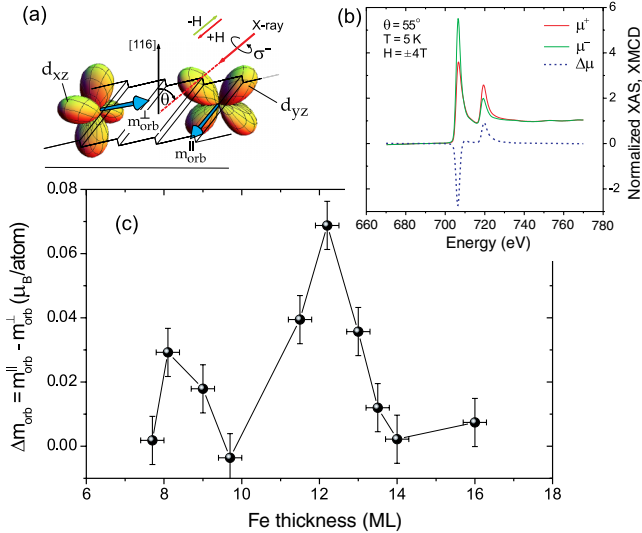


FIG. 4 (color online). (a) Schematics of XMCD measurement for Fe/Ag(116). The schematic view of d_{xz} and d_{yz} orbitals demonstrates the corresponding orientation of the orbital magnetic moments. (b) Normalized XAS spectra (μ^+ and μ^-) and XMCD spectra ($\Delta\mu$) for 9.7 ML thick Fe film. (c) The in-plane anisotropy of the orbital moment $\Delta m_{orb} = m_{orb}^{\parallel} - m_{orb}^{\perp}$ as a function of Fe thickness.

(Supplemental Material [13]). Within the perturbation theory approach [32,33], the components m_{orb}^{\parallel} and m_{orb}^{\perp} depend on the matrix elements of the orbital moment operators L_x and L_y , respectively. Since the elements $\langle \mu | L_x | \nu \rangle$ and $\langle \mu | L_y | \nu \rangle$ are finite for $\mu = d_{xy}$, $\nu = d_{yz}$, d_{zx} (while vanishing for $\mu = d_{yz}$, d_{zx} , $\nu = d_{yz}$, d_{zx}), the observed oscillations of m_{orb} for in-plane directions imply that they come from pairs of majority-spin states with one state of Δ_5 symmetry and the other of Δ_2' symmetry [d_{xy} in Fig. 1(c)]. Such pairs of states have vanishing elements of L_z , which explains the lack of oscillations of the orbital moment for the direction perpendicular to the sample plane. It also shows that pairs of states coming solely from the Δ_5 band (for which $\langle d_{zx} | L_z | d_{yz} \rangle \neq 0$) have a negligible contribution to the oscillatory orbital moment in the investigated Fe film.

In order to compare the orbital magnetic moment m_{orb} with magnetic anisotropy, it is more suitable to follow the anisotropy of the orbital moment rather than m_{orb} itself [37]. The dependence of the anisotropy of the in-plane orbital moment Δm_{orb} (i.e., the difference between m_{orb}^{\parallel} and m_{orb}^{\perp}) on Fe thickness is shown in Fig. 4(c). Two maxima in Δm_{orb} can be distinguished at ~ 8.4 ML and ~ 12.5 ML, i.e., at the same thicknesses of Fe (within the experimental error ± 0.3 ML), at which the maxima of H_s and PES intensity are observed. This highlights a correlation between the quantization of d_{xz} , d_{yz} orbitals, the anisotropy of the in-plane orbital moment Δm_{orb} , and the shift field H_s .

The anisotropy of the orbital moment is the sum $\Delta m_{orb} = \Delta m_{orb}^{\downarrow} + \Delta m_{orb}^{\uparrow}$ of contributions from the minority- and

majority-spin bands. They are related to the magneto-crystalline anisotropy energy via the approximate formula $\text{MAE} = -\alpha(\xi/4\mu_B)(\Delta m_{orb}^{\downarrow} - \Delta m_{orb}^{\uparrow})$ [32,33], where $\xi = 54$ meV is the spin-orbit coupling constant for Fe and the prefactor $\alpha = 0.05$ accounts for differences between microscopic and macroscopic probes of the MAE [38]. Simultaneously, the in-plane uniaxial magnetic anisotropy is well described by the equation $\text{MAE} = \mu_0 H_s M_s$ [29], where M_s is the saturation magnetization of bcc bulk Fe. Thus, the fact that the two maxima observed in the thickness dependence of Δm_{orb} [Fig. 4(b)] coincide with the maxima of H_s measured by MOKE (Fig. 3) confirms that the oscillations of Δm_{orb} and MAE result from the oscillatory dependence of $\Delta m_{orb}^{\uparrow}$, i.e., from the quantization of majority-spin states (see the Supplemental Material [13]). The two maxima of Δm_{orb} correspond to MAE values of $15.4 \mu\text{eV}/\text{atom}$ (at 8.4 ML) and $46.1 \mu\text{eV}/\text{atom}$ (at 12.5 ML), if the nonoscillatory contribution $\Delta m_{orb}^{\downarrow}$ is neglected. The analogous two maxima of H_s [Fig. 3] correspond to a change of magnetic anisotropy of $2.9 \mu\text{eV}/\text{atom}$ (at 9 ML) and $8.4 \mu\text{eV}/\text{atom}$ (at 13 ML). The difference in the oscillation amplitude value of MAE obtained in the two methods is most likely associated with inappropriate choice of the prefactor α , whose origin is not fully understood and which can be modified by the presence of atomic step edges [39]. The best agreement between the oscillation amplitude obtained from MOKE and XMCD is obtained for $\alpha = 0.01$. Note that in both H_s and Δm_{orb} dependencies, the maximum at ~ 8.4 ML is of much smaller amplitude than the maximum at ~ 12.5 ML. This is due to the proximity of the SRT thickness, at which the change in surface magnetic anisotropy reduces the in-plane uniaxial anisotropy [40].

As explained in the Supplemental Material [13], the observed oscillatory orbital magnetic moment in Fe/Ag(116) and oscillatory photoemission intensity in Fe/Ag(001) come from the same electronic orbitals since the oscillations of m_{orb} are found mostly for the direction perpendicular to the steps that corresponds to d_{xz} orbitals. The lobes of these orbitals lie in the vertical plane parallel to the steps so that their energies are only slightly modified, in comparison to those of Fe/Ag(001), by the presence of the stacking faults. This implies that the period of oscillations should be similar in both systems, indeed, what is observed in our experiments. It can be also argued (see the Supplemental Material [13]) that the existence of *in-plane* QWS due to the finite width of terraces on stepped surfaces [41] should not have a significant effect on the *out-of-plane* QWS observed in the present experiments.

Our PES results demonstrate that QWS can be clearly observed between 150 and 300 K, but previous MOKE experiments [6,30] found that MAE oscillations vanish above 200 K. The difference in the temperature dependence is due to the fact that MAE oscillations result not only from oscillations of the density of states itself but also require

that in each pair of coupled states contributing to MAE (i.e., Δ_5 and Δ'_2 in this case) one of them is located above E_F and the other below E_F . With increasing temperature, the thermal energy spread near E_F becomes comparable to the energy difference between the two states and, as a consequence, the MAE oscillations vanish [5,30].

Summarizing, we demonstrated that the magnetic anisotropy oscillations with increasing Fe film thickness are a direct consequence of the quantization of d states with Δ_5 spatial symmetry and majority-spin character. It is also found that the oscillations result from the coupling of these states with majority-spin states with Δ'_2 symmetry. We further show that the periodic contributions to the magnetic anisotropy due to QWS are governed solely by the in-plane orbital magnetic moments. The mechanism that we unveiled here can be extended to other magnetic materials, opening the possibility of tailoring magnetic anisotropy by appropriate electronic-structure engineering.

*Present address: Department of Physics and Astronomy, University of Pittsburgh, Pittsburgh, Pennsylvania 15260, USA.

mdabrows@mpi-halle.de

- [1] L. Joly, L. Tati-Bismaths, and W. Weber, *Phys. Rev. Lett.* **97**, 187404 (2006).
- [2] T. Niizeki, N. Tezuka, and K. Inomata, *Phys. Rev. Lett.* **100**, 047207 (2008).
- [3] Y. Z. Wu, A. K. Schmid, and Z. Q. Qiu, *Phys. Rev. Lett.* **97**, 217205 (2006).
- [4] D.-A. Luh, J. J. Paggel, T. Miller, and T.-C. Chiang, *Phys. Rev. Lett.* **84**, 3410 (2000).
- [5] M. Cinal, *J. Phys. Condens. Matter* **15**, 29 (2003).
- [6] J. Li, M. Przybylski, F. Yildiz, X. D. Ma, and Y. Z. Wu, *Phys. Rev. Lett.* **102**, 207206 (2009).
- [7] U. Bauer and M. Przybylski, *Phys. Rev. B* **81**, 134428 (2010).
- [8] U. Bauer, M. Dąbrowski, M. Przybylski, and J. Kirschner, *Phys. Rev. B* **84**, 144433 (2011).
- [9] Z.-Y. Lu, X.-G. Zhang, and S. T. Pantelides, *Phys. Rev. Lett.* **94**, 207210 (2005).
- [10] Z. Q. Qiu, J. Pearson, and S. D. Bader, *Phys. Rev. Lett.* **70**, 1006 (1993).
- [11] D. E. Bürgler, C. M. Schmidt, D. M. Schaller, F. Meisinger, R. Hofer, and H.-J. Güntherodt, *Phys. Rev. B* **56**, 4149 (1997).
- [12] R. K. Kawakami, E. J. Escorcia-Aparicio, and Z. Q. Qiu, *Phys. Rev. Lett.* **77**, 2570 (1996).
- [13] See the Supplemental Material at <http://link.aps.org/supplemental/10.1103/PhysRevLett.113.067203> for experimental details, results, and discussion of the XMCD measurements.
- [14] A. Winkelmann, D. Hartung, H. Engelhard, C.-T. Chiang, and J. Kirschner, *Rev. Sci. Instrum.* **79**, 083303 (2008).
- [15] J. Callaway and C. S. Wang, *Phys. Rev. B* **16**, 2095 (1977).
- [16] J. Schäfer, M. Hoinkis, E. Rotenberg, P. Blaha, and R. Claessen, *Phys. Rev. B* **72**, 155115 (2005).
- [17] W. Eberhardt and F. J. Himpsel, *Phys. Rev. B* **21**, 5572 (1980).
- [18] C. M. Schneider and J. Kirschner, *Crit. Rev. Solid State Mater. Sci.* **20**, 179 (1995).
- [19] M. El-Batanouny and F. Wooten, *Symmetry and Condensed Matter Physics. A Computational Approach* (Cambridge University Press, Cambridge, England, 2008).
- [20] Z. Q. Qiu and N. V. Smith, *J. Phys. Condens. Matter* **14**, R169 (2002).
- [21] N. V. Smith, *Phys. Rev. B* **32**, 3549 (1985).
- [22] W. Kuch and C. M. Schneider, *Rep. Prog. Phys.* **64**, 147 (2001).
- [23] R. Feder, A. Rodriguez, U. Baier, and E. Kisker, *Solid State Commun.* **52**, 57 (1984).
- [24] E. Vescovo, O. Rader, and C. Carbone, *Phys. Rev. B* **47**, 13051 (1993).
- [25] E. Kisker, K. Schröder, W. Gudat, and M. Campagna, *Phys. Rev. B* **31**, 329 (1985).
- [26] M. Pickel, A. B. Schmidt, F. Giesen, J. Braun, J. Minar, H. Ebert, M. Donath, and M. Weinelt, *Phys. Rev. Lett.* **101**, 066402 (2008).
- [27] M. Gradhand, M. Czerner, D. V. Fedorov, P. Zahn, B. Y. Yavorsky, L. Szunyogh, and I. Mertig, *Phys. Rev. B* **80**, 224413 (2009).
- [28] B. Ackermann, R. Feder, and E. Tamura, *J. Phys. F* **14**, L173 (1984).
- [29] W. Weber, C. H. Back, A. Bischof, C. Würsch, and R. Allenspach, *Phys. Rev. Lett.* **76**, 1940 (1996).
- [30] M. Przybylski, M. Dąbrowski, U. Bauer, M. Cinal, and J. Kirschner, *J. Appl. Phys.* **111**, 07C102 (2012).
- [31] J. Li, G. Chen, Y. Z. Wu, E. Rotenberg, and M. Przybylski, *IEEE Trans. Magn.* **47**, 1603 (2011).
- [32] P. Bruno, *Phys. Rev. B* **39**, 865 (1989).
- [33] G. van der Laan, *J. Phys. Condens. Matter* **10**, 3239 (1998).
- [34] T. Nakagawa, Y. Takagi, Y. Matsumoto, and T. Yokoyama, *Jpn. J. Appl. Phys.* **47**, 2132 (2008).
- [35] T. Yokoyama, T. Nakagawa, and Y. Takagi, *Int. Rev. Phys. Chem.* **27**, 449 (2008).
- [36] D. Weller, J. Stöhr, R. Nakajima, A. Carl, M. G. Samant, C. Chappert, R. Megy, P. Beauvillain, P. Veillet, and G. A. Held, *Phys. Rev. Lett.* **75**, 3752 (1995).
- [37] J. Stöhr and H. König, *Phys. Rev. Lett.* **75**, 3748 (1995).
- [38] A. N. Anisimov, M. Farle, P. Pouloupoulos, W. Platow, K. Baberschke, P. Isberg, R. Wäppling, A. M. N. Niklasson, and O. Eriksson, *Phys. Rev. Lett.* **82**, 2390 (1999).
- [39] S. S. Dhesi, G. van der Laan, E. Dudzik, and A. B. Shick, *Phys. Rev. Lett.* **87**, 067201 (2001).
- [40] M. Cinal, M. Dąbrowski, M. Przybylski, and J. Kirschner (unpublished).
- [41] J. E. Ortega, M. Corso, Z. M. Abd-el-Fattah, E. A. Goiri, and F. Schiller, *Phys. Rev. B* **83**, 085411 (2011).